J Sol-Gel Sci Technol (2007) 44:21–28
DOI 10.1007/s10971-007-1592-0

ORIGINAL PAPER

Sol–gel synthesis, characterization and photocatalytic activity of mesoporous TiO_2/γ-Al_2O_3 granules

Junseo Choi · Ji-Young Ban · Suk-Jin Choung · Jinsoo Kim · Haznan Abimanyu · Kye Sang Yoo

Received: 5 March 2007 / Accepted: 5 June 2007 / Published online: 12 July 2007

Abstract Mesoporous TiO_2/γ-Al_2O_3 composite granules were prepared by combining sol–gel/oil-drop method, using various titania solution. The product granules can be used as a photocatalyst or adsorbent in moving, fluidized bed reactors. The phase composition and pore structure of the granules can be controlled by calcination temperature and using different titania solution. In the photocatalysis of NH_3 decomposition, TiO_2/γ-Al_2O_3 granules using Degussa P25 powder treated thermally at 450 °C showed the highest catalytic ability. However, TiO_2/γ-Al_2O_3 granules using titania made by hydrothermal method had comparable performance in NH_3 decomposition.

Keywords TiO_2/γ-Al_2O_3 granules · Pore structure · Crush strength · Photocatalysis

1 Introduction

Ammonia decomposition process has been appealing a great interest in recent years. The decomposition reaction involves mainly producing controlled atmospheres for heat treatment in the metallurgical industry, for generation of the hydrogen–nitrogen mixture used in steel and electronic industries and eliminating an environmental pollution from the ammonia-containing waste gases [1–3]. In addition, the process of NH_3 decomposition is also attractive due to generation of CO*x*-free hydrogen for power proton exchange membrane fuel cells (PEMFC) and the unconverted NH_3 can be reduced to less than 200 ppb level by means of an adsorber [3, 4].

Homogeneous and heterogeneous photocatalyses have played an important role in many photochemical conversion processes, and have been extensively studied over the last two decades. Metal oxide materials including anatase TiO_2, WO_3, Ta_2O_5, and In_2O_3 have been widely investigated as the heterogeneous photocatalysts for the complete oxidation of toxic contaminants in liquid or gas phase [5–9]. In recent years, titania (titanium oxide) has been extensively studied and applied to degrading a wide range of organic compounds, for waste water treatment, and for abatement of bacteria [10–17]. TiO_2 photocatalytic materials are especially attractive because of its good properties such as non-toxic, clean and safe properties as well as high photocatalytic activity, thermal and chemical stability, and the abundance of the necessary raw materials [8, 18].

Unfortunately, pure titania exhibits low adsorption ability for the bulky organic pollutants. The quantum efficiency of this process proved to be quite low, which limited the practical application of this technique in industry [19]. However, the catalytic activity can be improved due to its deposition on inert porous supports. In recent years, attempts have been made to support fine TiO_2 on porous adsorbents like ordered mesoporous silica materials [20, 21].

Among several mesoporous ceramics, γ-alumina (γ-Al_2O_3) is probably the most common crystalline material extensively applied as a support body for catalysts or adsorbents due to its high surface area and abrasion

J. Choi · J.-Y. Ban · S.-J. Choung · J. Kim (✉)
College of Environment and Applied Chemistry, Kyung Hee University, 1 Seochen-dong, Giheung-gu, Yongin, Gyeonggi-do 449-701, Korea
e-mail: jkim21@khu.ac.kr

H. Abimanyu · K. S. Yoo (✉)
Energy and Environment Technology Division, Korea Institute of Science and Technology (KIST), 39-1 Hawolgokdong, Seongbukgu, Seoul 136-791, Korea
e-mail: kyoo@kist.re.kr

resistance. Preparation of porous metal oxide–alumina composite granules with desirable pore structure and admirable mechanical properties is of great worth to the development of novel catalysts and adsorbents for various applications. To our best knowledge, no significant work has been reported on the synthesis of TiO_2-Al_2O_3 composite granules with high surface area, controlled porosity and tailor-designed pore size distribution. Recently, we reported that mesoporous spherical TiO_2/γ-Al_2O_3 granules were prepared by an improved sol–gel/oil-drop granulation process [J. Choi, submitted]. The study concluded that the titania concentration is a critical factor for the shape and properties of the product composite granules. The pore structure of granules can be controlled by varying the concentration of TiO_2 and the calcination temperatures.

In this work, mesoporous TiO_2/γ-Al_2O_3 granules were prepared by the modified sol–gel/oil-drop process using various sources of titania as starting material, prepared by sol–gel method, hydrothermal method and using commercial product Degussa P25. Since titania particles prepared by different preparation techniques possess diverse properties, the product granules are also expected to show different pore structure, phase composition, and photocatalytic activity. In this paper, the structural and textural properties of the TiO_2/γ-Al_2O_3 granules as well as photocatalytic activity were systematically investigated.

2 Experimental

2.1 Preparation of TiO_2/Al_2O_3 granules

2 M stable boehmite sols were synthesized from hydrolysis and condensation of aluminum isopropoxide, AIP (Aldrich, MW = 204.25, 98% purity), using the modified Yoldas process as described in literature [22–24]. The precursor AIP was first hydrolyzed in 500 mL distilled water at 80~85 °C, and after 1 h of stirring, the resulting slurry (with AlOOH precipitates) was peptized with 1 M HNO_3, at an HNO_3 to AlOOH molar ratio of 0.07. The sol was refluxed overnight for more than 12 h at 95 °C to remove the remaining alcohol.

The titania sols were synthesized by three methods, sol–gel, hydrothermal and dispersing the commercial product Degussa P25 in water. 0.5 M titania sol was synthesized by hydrolysis and condensation of titanium tetraisopropoxide, TTIP (Aldrich, MW = 284.26, 97% purity) according to the literatures [25, 26]. TTIP was dissolved in isopropanol at room temperature and in a water-free atmosphere. Then, the solution was added slowly into the distilled water while stirring at high speed for 1.5 h, thus white precipitates formed. The precipitates obtained were separated and washed repeatedly with distilled water until the precipitates became free of alcohol. The precipitates were converted into a stable sol by dispersing in 1000 mL of water. 500 mL of well dissolved solution was followed by peptization with an addition of 1 M HNO_3 solution. Then, the solution was refluxed at 80 °C for 12 h. To obtain 0.5 M titania solution by hydrothermal method, TTIP in isopropanol and water were poured into an autoclave of Morey type with Teflon® chamber (Ø 80 mm × H 120 mm, volume 450 mL) and treated hydrothermally at 120 °C for a reaction time of 12 h in accordance with literature [23]. As the third method for titania solution, commercial catalysts Degussa P25 powder (50 m^2/g; 15~30% rutile + 85~70% anatase, mean diameter of 30 nm) was dispersed in water at room temperature for 0.5 h.

The obtained boehmite sol and various titania solutions were respectively mixed with a fixed volume ratio of 5:1 and dispersed using ultrasonic homogenizer (500 watt, Cole-Parmer) with a 50% pulse for 0.5 h. The sol mixtures were stirred at room temperature for 0.5 h. Then, a small amount of 1 M HNO_3 was added into the sol mixtures and heated up to 70 °C under vigorous stirring. These partially gelled sols were transferred into droppers for generating of sol droplets of about 5 mm in size. The droplets fell through a liquid bath consisting of a paraffin oil layer (mineral oil, from Yakuri Pure Chemicals Co. Ltd.) and a 10 wt% ammonia solution layer as described in the literature [22, 23]. The obtained granules were calcined at various temperatures of 450, 600, and 750 °C for 3 h at a heating rate of 1 °C /min. The product composite granules using titania solutions prepared by sol–gel method, hydrothermal method and using P25 powders were labeled as SG, HT and P25, respectively.

2.2 Characterization of synthesized granules

The shape and size of the TiO_2/γ-Al_2O_3 granules were observed using an optical microscope (Microscope System STVMS 305R, Sometech). A universal testing instrument (Universal Electron mechanical Testing Systems 5800 series, Instron) was used to evaluate the crush strength of the different granular particles, which were taken as the maximum load applied to break the granules. The crush strength data obtained by the universal testing instrument used on TiO_2/γ-Al_2O_3 granules were reproduced at least 15 times within an error of about 20%.

For the identification of crystallinity, an X-ray diffractometer (M18XHF-SRA, Mac Science) was used with Ni filtered CuK_α (λ = 1.54056 Å) radiation over the range 2θ from 20 to 80°, with a scanning speed of 1°/min. The crystallite sizes (D_{hkl}) were calculated using the Scherrer relationship [27].

The specific surface area (SSA), pore size distribution (PSD) and pore volume of the TiO_2/γ-Al_2O_3 granules were obtained by N_2 adsorption/desorption at 77 K using Micromeritics ASAP2020 equipment. All granules were degassed at 150 °C for 1 h prior to measurement. The specific surface area was determined by the multipoint Brunauer-Emmett-Teller (BET) method using the adsorption data in the relative pressure (P/P_0) range of 0.05~0.25. The pore size distribution data were calculated by the ASAP 2020 software from the N_2 desorption isotherms. The Barrett-Joyner-Halender (BJH) method with cylindrical pore size calculated from the Kelvin equation was used in the data processing.

2.3 Analysis of NH_3 decomposition in photocatalytic batch systems

To determine the photocatalytic performance of the TiO_2/γ-Al_2O_3 granules, NH_3 decomposition was conducted using a batch photo-reactor system, as shown in Fig. 1. A quartz cylinder with dimensions of 15.5 cm in length and 0.35 cm in diameter was used as a reactor. About 5 mL of TiO_2/γ-Al_2O_3 granules were filled into quartz cylinder reactor. Four UV-lamps (model UV-A, 365 nm, 15 W/cm^2, 20 cm length × 1.5 cm diameter, Sankyo, Japan) were used for photocatalytic reaction. The initial NH_3 concentration was fixed to 1000 ppm.

During the photocatalytic decomposition of NH_3, the products were analyzed using gas-chromatograph equipments (GCs) of HP 5890 Series II with FID- and TCD detector types. To determine the exact by-products and intermediates, the GCs were connected directly to the photo-reactor during the NH_3 decomposition processes.

3 Results and discussion

The amount of TiO_2 concentration is an important factor for the shape and properties of the product granules. In other words, gelation time becomes longer with increasing TiO_2 concentration, resulting in smaller granule size and weaker mechanical strength of granules. After being dried, all granules shrank 50~70% in size and showed much improved mechanical strength. The granules are spherical with a diameter of ca. 1~2 mm. Figure 2 shows the optical photographs of TiO_2/Al_2O_3 granules using TiO_2 solutions prepared by various methods. It can be seen that SG granules (Fig. 2a) are very spherical compared to the other granules (Fig. 2b, c). HT granules are better than P25 granules. The granules made using commercial TiO_2 (Degussa P25) are the worst with irregular size and shape.

Table 1 illustrates the specific surface area, pore volume and average pore diameter of the granules at various calcination temperatures. The surface area and the crush strength of SG granules are greater than those of HT and P25 granules. An increase of calcination temperature from 450 to 750 °C deteriorated the surface area of all granules about 33%. The pore volume of SG, HT and P25 granules decreased, respectively, from 0.50 to 0.48, from 0.49 to 0.48 and from 0.45 to 0.41 cm^3/g. The pore diameters of SG and HT granules were increased upon heat treatment from 450 to 750 °C, respectively, around 48% and 43%.

Figure 3 shows crush strength of the granules against the calcination temperatures. SG granules possess higher crush strength than the others at all calcination temperatures. The crush strength of SG granules decreased from 154 N to 139 N, as the calcination temperature was increased from 450 °C to 600 °C. However, an increase of temperature to 750 °C decreased the crush strength slightly to 135 N. Meanwhile, the HT granules show a gradual decrease of crush strength with calcination temperature. It declined from 130 N at 450 °C to 109 N at 750 °C and 93 N at 750 °C. TiO_2 and/or γ-Al_2O_3 particles are grown into larger crystals with the calcination temperature and bond together strongly to form a solid arrangement. The crush strength of SG and HT granules also became smaller with increasing calcination temperature because of an increase of pore diameter (see Table 1). It is noteworthy that

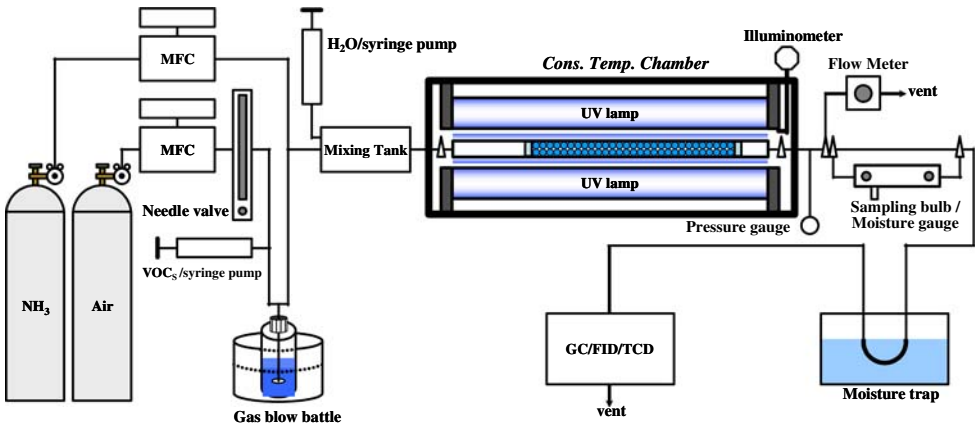

Fig. 1 Scheme of photocatalysis system for the decomposition of NH_3

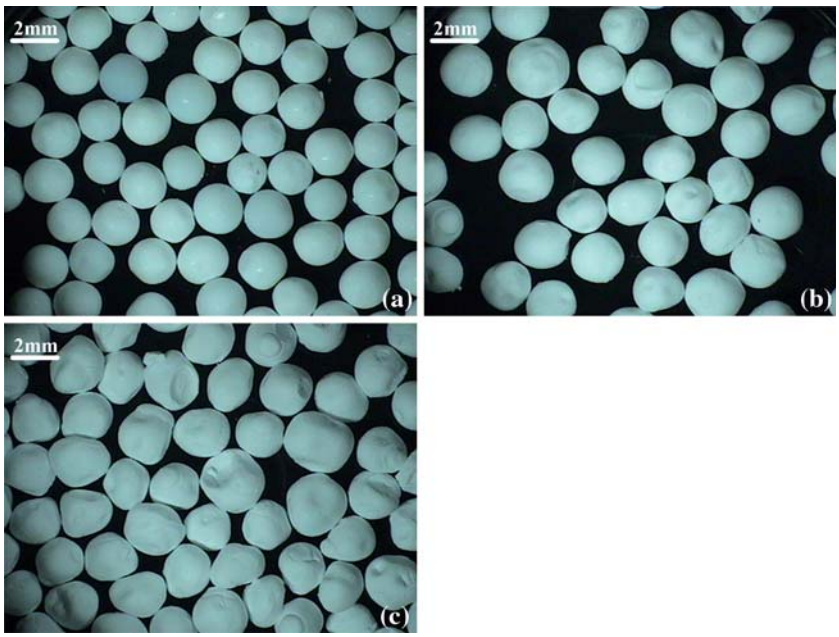

Fig. 2 Optical photograph of TiO_2/γ-Al_2O_3 granules using TiO_2 by (**a**) sol–gel method, (**b**) hydrothermal method, and (**c**) Degussa P25

Table 1 Pore structure data of various TiO_2/Al_2O_3 granules as a function of calcination temperature

Pore structure data	Calcination Temperature								
	450 °C/3 h			600 °C/3 h			750 °C/3 h		
	SG	HT	P25	SG	HT	P25	SG	HT	P25
SSA (m^2/g)	285	273	201	237	221	173	192	184	134
Pore volume (cm^3/g)	0.50	0.49	0.45	0.51	0.50	0.44	0.48	0.48	0.41
Pore diameter (nm)	4.6	4.9	6.0	5.7	5.9	6.7	6.8	7.0	8.3

the crush strength of P25 granules was increased with increasing the calcination temperature. It might be attributed to the fact that the P25 powders maintained the similar crystallite size and phase composition with calcination temperature. It should be noted that the crush strength of granules prepared in this study is better than the commercial γ-alumina granules (about 25 N/granule) [23].

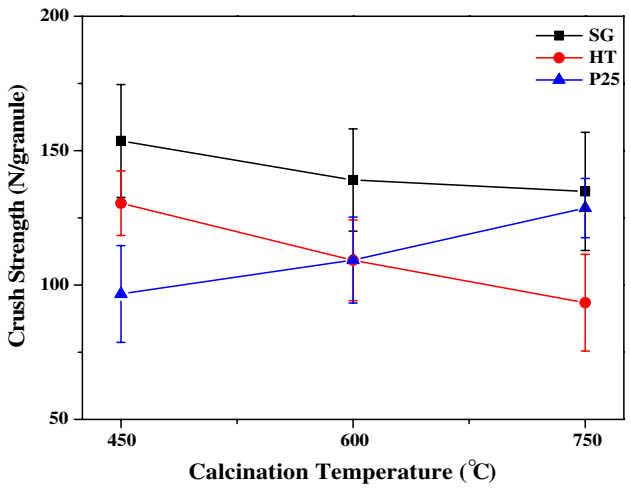

Fig. 3 Plots of crush strength of TiO_2/γ-Al_2O_3 granules over calcination temperatures

The effect of various TiO_2 solutions (by sol–gel method, hydrothermal method and using Degussa P25) on phase structure was investigated by XRD analysis. The uncalcined Al_2O_3 granules usually show a diffraction pattern of boehmite crystalline indicated dominant by the Miller indices of (021), (130), (002) and (200). Further calcinations above 450 °C not only consolidated the granules, but also facilitated the phase transformation from boehmite to γ-Al_2O_3 [28, 29]. Similarly, heat treatment of TiO_2 powder not only consolidated the particles but also facilitated the phase transformation from amorphous to metastable anatase and then to stable rutile phase [25, 26]. Figure 4 shows the XRD patterns of TiO_2/γ-Al_2O_3 granules with various TiO_2 solutions after calcination at 450, 600 and 750 °C. It was observed that the crystallinity of the TiO_2 particles increased with increasing calcination temperature. The XRD patterns of SG granules (Fig. 4a) showed both anatase phase ($2\theta = 25°$) and γ-Al_2O_3 phase ($2\theta = 37°$, 47° and 67°) after calcination at 450 °C, and these phases were maintained at 750 °C. After calcinations at 450 and

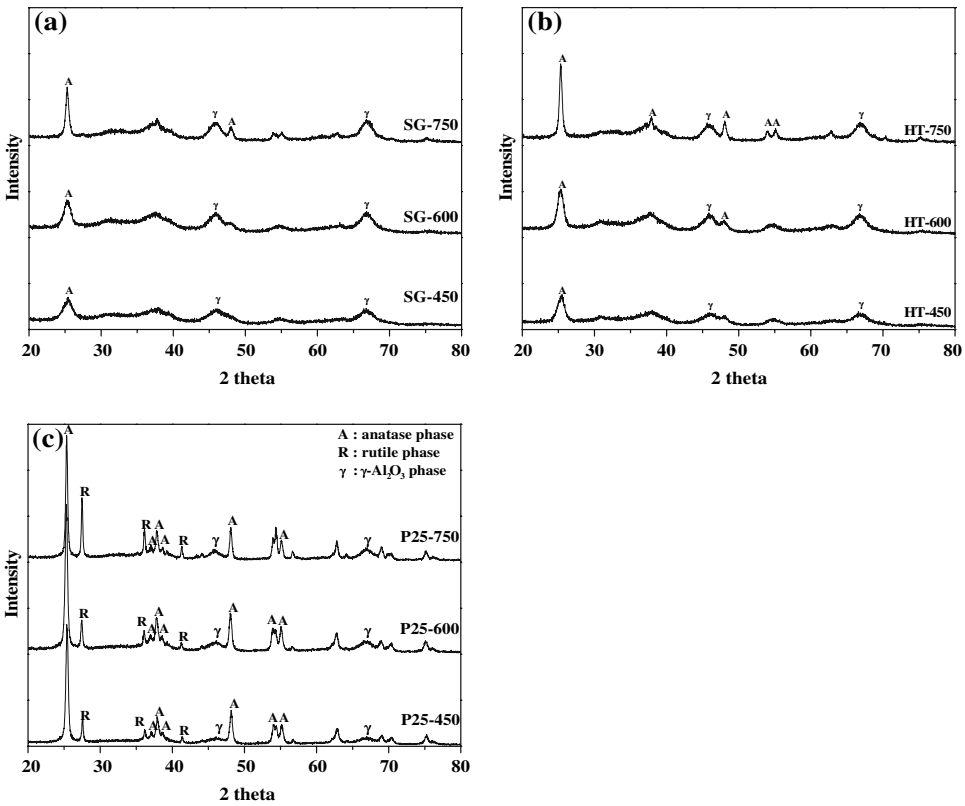

Fig. 4 XRD patterns of TiO_2/γ-Al_2O_3 granules using TiO_2 by (**a**) sol–gel method, (**b**) hydrothermal method and (**c**) Degussa P25 at various calcination temperatures

600 °C, HT granules (Fig. 4b) showed the similar XRD pattern with that of SG granules. However, at 750 °C the peaks at $2\theta = 38$, 48, 54 and 55° became more sharp indicating crystallite growth. Generally, anatase-to-rutile phase transformation started to occur after calcinations above 600 °C, but it didn't occur after calcination at 750 °C in this study. The absence of rutile phase in the XRD patterns of SG and HT granules indicates that the granules seized very small crystallite size. The pore volume and surface area of the particles were not small enough to initiate the nucleation of rutile by increasing contact points between anatase crystals. On the other hand, P25 granules (Fig. 4c) showed both anatase phase and rutile phase at all calcination temperatures. The weight fraction of the rutile phase increased from 21.3% to 38.2% with increasing the calcination temperature from 450 °C to 750 °C. However, aluminum titanate (Al_2TiO_5) was not found in all samples. This phase composition evolution is in agreement with Yang et al [30].

Figure 5 shows the isotherms and pore size distributions of the TiO_2/γ-Al_2O_3 granules after calcination at 450 °C. According to BDDT classification [31], all granules show isotherms of type IV, which exhibit hysteresis loops mostly of H2 and H3. This indicates that the granules contain mesopores (2~50 nm) with both narrow slit-shaped pores and ink-bottle pores. Also, the isotherms show one hysteresis loops, showing monomodal pore size distributions in the mesoporous region (2~10 nm). The pore size distributions of the granules were calculated from the desorption branch of the isotherms. In sol–gel process, the primary particles of uniform size are formed by hydrolysis and condensation processes and then connected together to form aggregates during gelation. During calcinations, these primary particles are grown into larger crystals and bounded together tightly to form a solid network, resulting in a narrow pore size distribution [32]. On the other hand, the basic mechanism for the hydrothermal formation of ceramic oxide particles involves a dissolution-precipitation mechanism. Nucleation is accelerated due to water, and the secondary particles are dissolved by dissolution-precipitation mechanism. So, pores between secondary particles are disappeared, resulting in a narrow pore size distribution [22, 23, 33]. In contrast, Degussa P25 powders were prepared at elevated temperature (>1000 °C) by flame synthesis, resulting in larger crystalline anatase and rutile powders. Therefore, P25 granules have the widest pore diameter region of 2.0~11.5, whereas SG and HT granules have narrow pore diameter region of 2.0~6.5 and 2.0~8.5.

Figure 6 shows the isotherms and pore size distributions of the TiO_2/γ-Al_2O_3 granules after calcination at 750 °C. The adsorption isotherms are type IV according to the BDDT classification. It is observed that the low relative pressure point, where the adsorption and desorption branches coincide, is affected by the calcination temperature of

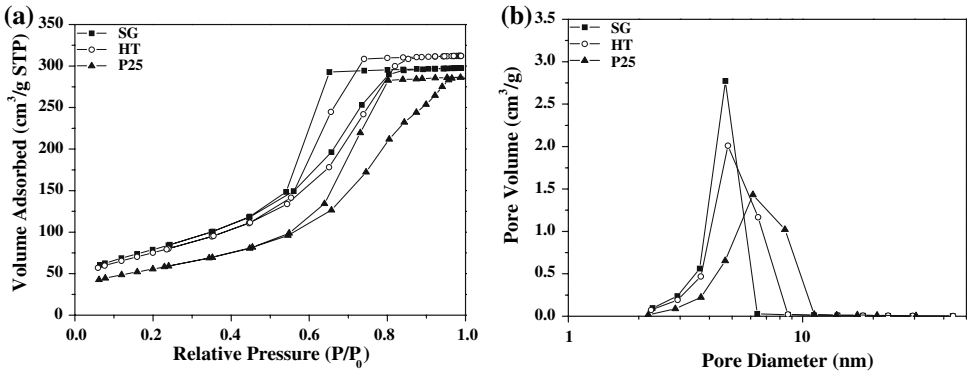

Fig. 5 Isotherms (**a**) and Pore size distributions (**b**) of TiO_2/γ-Al_2O_3 granules after drying and calcination at 450 °C for 3 h

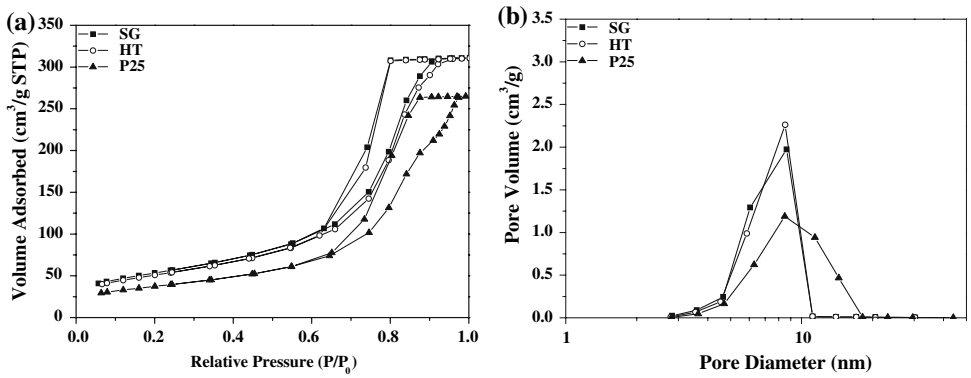

Fig. 6 Isotherms (**a**) and Pore size distributions (**b**) of TiO_2/γ-Al_2O_3 granules after drying and calcination at 750 °C for 3 h

the samples. The adsorption isotherms appear at higher relative pressures (≥0.65) as the severity of the treatment increases, indicating the occurrence of capillary condensation at larger pores. The pore size distributions are monomodal and move toward larger pores (≥3 nm) with increasing calcination temperature of the samples. Thus, P25 granules calcined at 750 °C have the largest pore diameter of 8.3 nm, whereas SG granules calcined at 750 °C have the smallest pore diameter of 6.8 nm.

The anatase crystallite sizes are shown in Fig. 7 as a function of calcination temperature for various TiO_2/γ-Al_2O_3 granules. The anatase crystallite size of all TiO_2/γ-Al_2O_3 granules became larger with increasing calcination temperature. The increase in the crystallite size was slow at 450–600 °C. Then, it increased drastically in the temperature range from 600 to 750 °C. The anatase crystallite size of P25 granules is larger than that of the other TiO_2/γ-Al_2O_3 granules at all calcination temperatures. On the other hand, the anatase crystallite sizes of SG granules were the smallest at all calcination temperatures. P25 granules calcined at 750 °C possessed the largest anatase crystallite size of 27 nm, whereas SG granules calcined at 450 °C had the smallest anatase crystallite size of 10 nm.

Plots of the decomposition of NH_3 with respect to reaction time over various TiO_2/γ-Al_2O_3 granules after calcinations at 450 °C and 750 °C are shown in Fig. 8a, b, respectively. At calcination temperature of 450 °C (Fig. 8a), HT and P25 granules show good catalytic activity with NH_3 conversion respectively of 95% and 92% in 20 min, while the conversion of 100% was achieved in 40 min. However, SG granules converted NH_3 only 35% in 20 min and achieved almost 100% conversion in 100 min. On the other hand, at calcination temperature of 750 °C (Fig. 8b), the catalytic activity of SG granules is the best

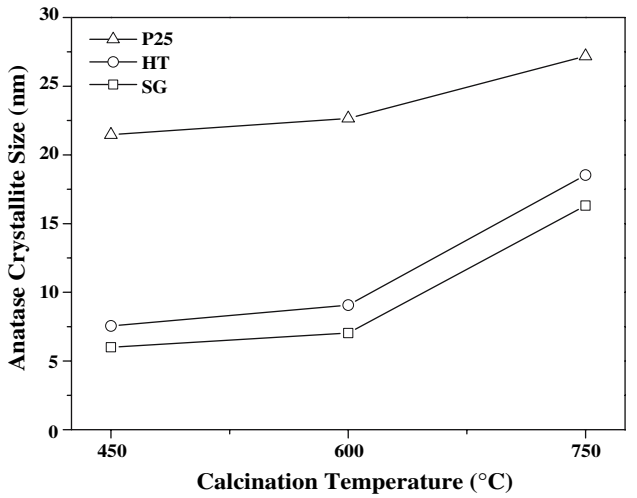

Fig. 7 Anatase crystallite sizes of TiO_2/γ-Al_2O_3 granules after calcination at 450, 600, 750 °C for 3 h

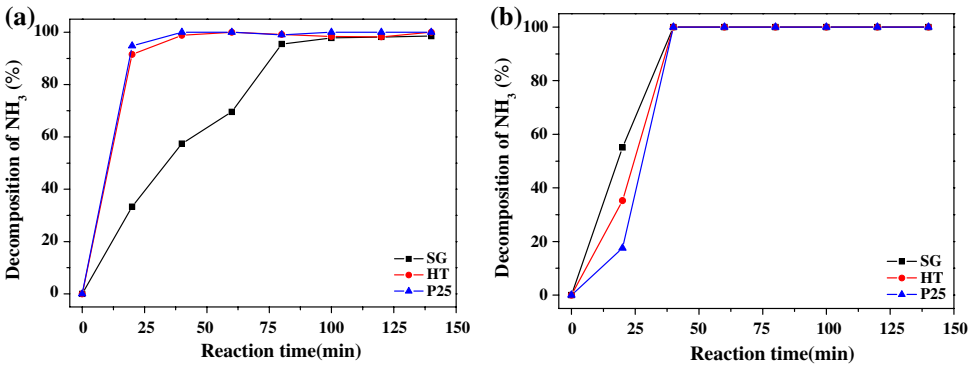

Fig. 8 Photocatalytic performance as a function of reaction time for NH_3 removal over the TiO_2/γ-Al_2O_3 granules after calcination for 3 h at (**a**) 450 °C and (**b**) 750 °C

with NH_3 conversion about 55% in 20 min. Meanwhile, HT and P25 granules achieved in the same time NH_3 conversion about 35% and 17%, respectively. However, all granule types converted NH_3 conversion 100% in 40 min. Generally, the catalytic performance of TiO_2 is influenced by anatase phase. P25 granules calcined at 450 °C could obtain the highest NH_3 decomposition since they seized more anatase crystalline. Although P25 granules calcined at 750 °C had also anatase phase, their activity became worse due to the increase of rutile phase from 21.3% to 38.2%. On the other hand, SG granules calcined at 750 °C showed the highest NH_3 decomposition possibly because of largest specific surface area and the smallest pore diameter.

4 Conclusions

Mesoporous spherical TiO_2/γ-Al_2O_3 granules were prepared by modified sol–gel granulation process using various titania solution. In this preparation, the type of titania solution and calcination temperature were critical factors to determine the shape and properties of the product granules. The surface area of granules decreased with calcination temperature, but pore diameter increased. Crush strength of granules was also affected by calcination temperature. For photocatalysis experiments, the catalytic performance was determined mainly by titania solution. TiO_2/γ-Al_2O_3 granules with P25 titania solution calcined at 450 °C showed the best result in NH_3 decomposition due to anatase presence in the granules. However, TiO_2/γ-Al_2O_3 granules with sol–gel titania solution calcined at 750 °C showed the highest NH_3 decomposition presumably due to highest specific surface area and fine pore size.

Acknowledgments The authors wish to acknowledge the financial support from MOST of Korea and KAERI. This work has been partially carried out under the Nuclear Hydrogen Development and Demonstration project (NHDD).

References

1. Liang C, Li W, Wei Z, Xin Q, Li C (2000) Ind Eng Chem Res 39:3694
2. Hashimoto K, Toukai N (2000) J Mol Catal A Chem 161:171
3. Choudhary TV, Sivadinarayana C, Goodman DW (2001) Catal Lett 72:197
4. Chellappa AS, Fischer CM, Thomson WJ (2002) Appl Catal A: Gen 227:231
5. Herrmann J-M (1999) Catal Today 53:115
6. Vautier M, Guillard C, Herrmann J-M (2001) J Catal 201:46
7. Hu C, Wang Y, Tang H (2001) Appl Catal B Env 35:95
8. Hoffmann MR, Mrtin ST, Choi WY, Bahnemann DW (1995) Chem Rev 95:69
9. O'shea KE, Beightal S, Garcia I, Aguilar M, Kalen DV, Cooper WJ (1996) J Photochem Photobiol A: Chem 107:221
10. Tanaka K, Abe K, Hisanaga T (1996) J Photochem Photobiol A: Chem 101:85
11. Bauer R, Waldner G, Fallmann H, Hager S, Klare M, Krutzler T, Malato S, Maletzky P (1999) Catal Today 53:131
12. Devahasdin S, Fan C, Li K, Chen DH (2003) J Photochem Photobiol A: Chem 156:161
13. Ao CH, Lee SC, Yu JZ, Xu JH (2004) Appl Catal B: Environ 54:41
14. Parra S, Malato S, Pulgarin C (2002) Appl Catal B: Environ 36:131
15. Gumy D, Morais C, Bowen P, Pugarin C, Giraldo S, Hajdu R, Kiwi J (2006) Appl Catal B: Environ 63:76
16. Lee B, Park S, Kang M, Lee S, Choung S (2003) Appl Catal A: Gen 253:371
17. Sopyan I, Watanabe M, Murasawa S, Hashimoto K, Fujishima A (1996) J Photochem Photobiol A: Chem 98:79
18. Hagfeldt A, Gratzel M (2000) Acc Chem Res 33:269
19. Dionysiou DD, Suidan MT, Bekou E (2000) Appl Catal B 26:153
20. Bhattacharyya A, Kawi S, Ray MB (2004) Catal Today 98:431
21. Sun D, Liu Z, He J, Han B, Zhang J, Huang Y (2005) Microp Mesop Mater 80:165
22. Buelna G, Lin YS (1999) Microp Mesop Mater 30:359
23. Buelna G, Lin YS, Liu X, Lister JD (2003) Ind Eng Chem Res 42:442
24. Deng SG, Lin YS (1997) AIChE J 43:505

25. Kim J, Wklhelm O, Pratsinis SE (2001) J Am Ceram Soc 84:2802
26. Kim J, Song KC, Foncillas S, Pratsinis SE (2001) J Eur Ceram Soc 21:2863
27. Cullity BD (1978) Elements of X-Ray Diffraction, 2nd edn. Addison-Wesley, Reading, p 86
28. Leenaars AFM, Burggraaf AJ (1984) J Mater Sci 19:1077
29. Wilson SJ, Stacey MH (1981) J Coll Int Sci 82:507
30. Yang J, Huang YX, Ferreira JMF (1997) J Mater Sci Lett 16:1933
31. Sing KSW, Everett DH, Haul RAW, Moscou L, Pierotti RA, Rouquerol J, Siemieniewska T (1985) Pure Appl Chem 57:603
32. Brinker CJ, Scherer GW (1990) Sol–gel science: the physics and chemistry of sol–gel processing. Academic Press, New York
33. Chu L, Hsiue G, Lin I (2006) Acta Mater 54:1671